Nanostripe length dependence of plasmon-induced material deformations

Ventsislav K. Valev,[1,*] Wim Libaers,[2] Urs Zywietz,[3] Xuezhi Zheng,[4] Marco Centini,[5] Nils Pfullmann,[6,7] Lars O. Herrmann,[1] Carsten Reinhardt,[3] Vladimir Volskiy,[4] Alejandro V. Silhanek,[8] Boris N. Chichkov,[3] Concita Sibilia,[5] Guy A. E. Vandenbosch,[4] Victor V. Moshchalkov,[9] Jeremy J. Baumberg,[1] and Thierry Verbiest[2]

[1]*Nanophotonics Centre, Cavendish Laboratory, University of Cambridge, Cambridge CB3 0HE, UK*

[2]*Molecular Electronics and Photonics, INPAC, KU Leuven, Leuven BE-3001, Belgium*

[3]*Laser Zentrum Hannover e.V., Hanover D-30419, Germany*

[4]*SAT-TELEMIC, KU Leuven, Leuven BE-3001, Belgium*

[5]*Dipartimento di Scienze di Base e Applicate per l'Ingegneria (SBAI), SAPIENZA Università di Roma, Roma 16 00161, Italy*

[6]*Leibniz Universität Hannover, Institut für Quantenoptik, Welfengarten 1, Hannover D-30167, Germany*

[7]*QUEST, Centre for Quantum Engineering and Space-Time Research, Hannover, Germany*

[8]*Département de Physique, Université de Liège, Sart Tilman BE-4000, Belgium*

[9]*Superconductivity and Magnetism & Pulsed Fields Group, INPAC, KU Leuven, Leuven BE-3001, Belgium*

**Corresponding author: vkv23@cam.ac.uk*

Received November 19, 2012; revised March 20, 2013; accepted May 29, 2013;
posted May 29, 2013 (Doc. ID 180209); published June 24, 2013

Following the impact of a single femtosecond light pulse on nickel nanostripes, material deformations—or "nanobumps"—are created. We have studied the dependence of these nanobumps on the length of nanostripes and verified the link with plasmons. More specifically, local electric currents can melt the nanostructures in the hotspots, where hydrodynamic processes give rise to nanobumps. This process is further confirmed by independently simulating local magnetic fields, since these are produced by the same local electric currents. © 2013 Optical Society of America

OCIS codes: (240.6680) Surface plasmons; (260.7120) Ultrafast phenomena.
http://dx.doi.org/10.1364/OL.38.002256

In the last decade, metallic nanostructures have been shown to exhibit remarkable optical properties, with very important impact on a variety of scientific disciplines, such as medicine [1], chemistry [2,3], and physics [4,5]. In material science and engineering, metallic nanostructures, which are at the basis of metamaterials, have opened the way for all optical communication [6,7], cloaking [8], and the perfect lens [9,10]. In all of these instances, one of the main properties of metallic nanostructures, which is behind new concepts and applications, is the surface plasmon resonance.

Surface plasmons are coherent electron oscillations, which can occur in metallic nanostructures, for visible light excitation. One of the reasons that light can efficiently excite surface plasmons resides in the fact that the electric field component of light can induce charge polarization at the surface of the nanostructures. In a perfectly spherical nanoparticle, with a radius much smaller than the wavelength, the electron cloud is essentially pushed away from the direction of the electric field of light, and it oscillates in response to the frequency of light. Should this nanostructure become elongated, it would form a resonant cavity, whereby, depending on the wavelength of light and on the length of the nanostructure, consecutive plasmon resonance modes would be excited. In highly absorbing materials, such as nickel, the plasmonic currents bounce from the edges and can result in reinforced hotspots, whereas hotspots toward the middle of the nanostructure can be attenuated due to absorption of the plasmonic currents. Because these resonance modes govern the optical properties of nanostructures, recently, a considerable effort has been devoted to their experimental visualization. For instance, cathodoluminescence [11] and electron energy loss spectroscopy [12] both offer the high resolution of a scanning electron microscope, though they can only be used in vacuum. An alternative can be found in apertureless, scanning near-field scattering-type optical microscopy (*s*-SNOM) [13], although the interaction between the tip of the microscope in this case can be an important complication.

Two years ago, a new method for visualizing near-field excitations in metallic nanostructures was proposed, whereby ultrafast laser pulses can be employed to imprint the pattern of the near field on the surface of the nanostructures [14]. It was immediately apparent that the method could be very promising for visualizing plasmons, combining speed, robustness, and ease of use. Then, a few months later, it was demonstrated that the imprints are due to hydrodynamic processes occurring in metallic nanostructures under the impact of ultrafast laser pulses [15]. This demonstration was performed for a single laser wavelength, on fairly complex, *G*-shaped nanostructures.

In order to unambiguously demonstrate the sensitivity of the imprinting method to plasmons, here, we present a study of very straightforward geometries: nanostripes. Upon varying the length of these nanostripes, different plasmon modes are excited, resulting in different nanobumps in the nanostructures. By comparing these nanobumps to rigorous numerical simulations, we show that, following charge separation, local electron currents are responsible for raising the temperature of the nanostructures. Moreover, the oscillation of these charges gives rise to local magnetic fields, which coincide with both the maxima in electric currents and the regions of temperature increase in the samples.

The samples were prepared by electron beam lithography following the method described in [16]. The overall geometry is that of a nanostripe, with dimensions indicated in the scanning electron microscopy (SEM) micrographs. The nanostructures were deposited on a substrate made of SiO_2 (100 nm) on top of Si (001). A Cr (5 nm) adhesion layer was used, prior to the deposition of the nanostructures, which were made of Ni (35 nm), as this is a strongly absorbing material, well suited for imprinting. The nanostructures were separated by a distance of 1000 nm, edge to edge, in order to ensure that they do not influence each other upon illumination. Figure 1(a) presents a schematic diagram of the experimental configuration. The illumination was performed with single ultrafast laser pulses (60 fs), at a wavelength of 800 nm and at normal incidence. The illumination area on the sample was a square of 6 by 6 μm; i.e., it covered all the nanostructures. Other details on the laser chain and the optical setup can be found in [15].

In our experiments, the energy of the laser pulses ($1.4 \cdot 10^{12}$ W/cm^2) is not sufficient to melt the nanostructures. However, due to plasmon excitation and near-field enhancement in the hotspots, melting can occur locally, as demonstrated by the numerical simulations of temperature in Figs. 1(b) and 1(c). The temperature distribution within these nanostripes is governed by the heat source density [17]. The latter was determined via finite-difference time-domain calculations based on open source implementation of MEEP [18]. Subsequently, the diffusion equation was solved to obtain the temperature increase. Within the hotspots, this temperature increase gives rise to hydrodynamic processes. As a consequence, nanobumps appear in the nanostructures, as shown in the SEM image in Fig. 1(d). The exact nature of the hydrodynamic processes that produce nanobumps is under discussion [19,20]. Because these nanobumps are not easily distinguished upon observation from the top, SEM was performed at 45°. From this angle, a very clear shape deformation of the nanostructure can be observed; the nanostructure appears to bend upward, in the middle of the front side. An identical shape deformation is situated on the opposite side of the nanostructure, although it is not clearly distinguishable, due to the tilt of the SEM image. These nanobumps are due to the impact of single femtosecond pulses with polarization parallel to the length of the nanoparticle. Similar nanobumps can be seen for a polarization perpendicular to the length of the nanoparticle, as illustrated in Fig. 1(e). Because these nanobumps are not situated in the corners of the nanostripes, they are more likely to be associated with plasmons than with the lightning rod effect. Moreover, in this type of structure, plasmons are well known to depend on the length of the nanostripes. What then is the effect of increasing the nanostructures' length?

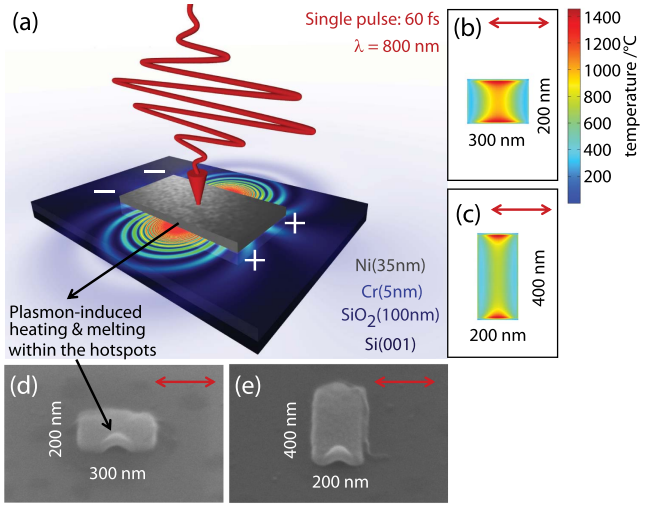

Fig. 1. (a) Schematic diagram of the experimental configuration. The electric field of light causes charge separation in the nanostructure, and the associated local electric current oscillations induce heating and melting in the hotspots. The temperature increase in these hotspots is evaluated by numerical simulations in (b) and (c), where the direction of linear polarization is indicated with a double arrow. The melting results in the formation of nanobumps, as shown by the SEM image in (d). For a polarization oriented perpendicularly to the nanostructures, the position of the nanobumps is shown in (e).

In Fig. 2, four nanostructures with different length have been studied. The figure shows SEM images, again performed at 45°, of the four nanostructures. The images were taken following single pulse illumination, with the direction of light polarization parallel and perpendicular to the nanostructures, in Figs. 2(a) and 2(b), respectively. In each case, the direction of polarization is indicated with double arrows on the figure. It is immediately apparent that, for parallel polarization and a length of 750 nm, there are only two nanobumps, situated in the middle, just as is the case in Fig. 1(b). However, for a nanostructure with 900 nm length, there is a difference in the nanobump pattern, whereby four nanobumps can now be observed. These four nanobumps remain visible for lengths of 1100 and 1200 nm. At variance, in the case of a polarization perpendicular to the nanostructures, the pattern of nanobumps remains the same regardless of the lengths. The origin of the nanobump patterns can be investigated with numerical simulations [21].

Because the nanobumps are attributed to local melting of the nanostructures, which is caused by local electric currents, we simulated the distribution of such currents in four nanostripes with identical dimensions to those in Fig. 2. These simulations were performed with MAGMAS [22,23], for a plane wave illumination at 800 nm, and the

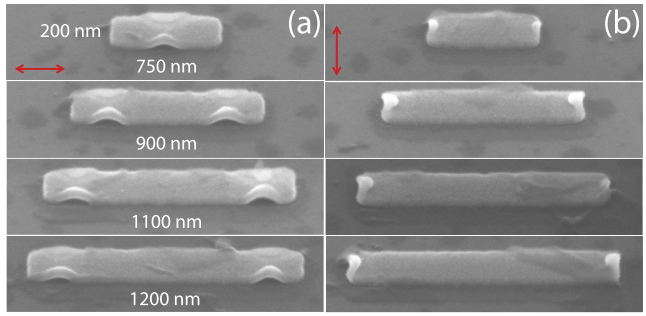

Fig. 2. For incident light with 800 nm wavelength, different plasmon modes are excited, depending on the dimensions of the nanostructures. In (a) SEM shows the pattern of nanobumps that are induced by single light pulses with polarization oriented along the nanostructures. The nanobumps that are induced for perpendicular polarization are shown in (b).

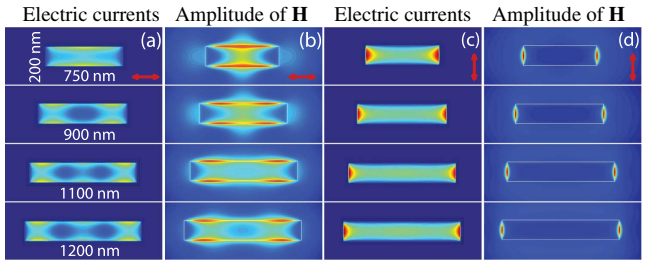

Fig. 3. Both the positions of local electric currents and the induced magnetic fields in the nanostructures match the pattern of the nanobumps. For the case of incident light, polarized along the nanostructures, numerical simulations of the local electric current and of the induced magnetic fields are shown in (a) and (b), respectively. For the case of light polarization perpendicular to the nanostructures, the local electric currents and the induced magnetic fields are presented in (c) and (d), respectively.

results are shown in Figs. 3(a) and 3(b), for light polarization parallel and perpendicular to the nanostructures, respectively. The simulations demonstrate that there is an unambiguous match between the maxima of local electric currents and the nanobumps.

Next, in order to test the robustness of our results, we performed independent simulations of the local magnetic fields in the nanostructures. Indeed, just as the local electric currents cause local heating, they also induce local magnetic fields. Consequently, the positions of the maximal local magnetic field amplitude should coincide with the positions of the maximal local currents and with the nanobumps. The magnetic fields were simulated with Lumerical, for a plane wave at 800 nm, and the results are displayed in Figs. 3(c) and 3(d), for the case of light polarization parallel and perpendicular to the nanostructures, respectively. These results are in excellent agreement with our expectations.

In conclusion, we have studied the nanostripe length dependence of plasmon-induced nanobumps, in the case of nickel nanostructures. The pattern of nanobumps is related to the plasmon behavior. Nanobumps occur in the regions of high electric currents, which are responsible for local melting and hydrodynamic processes. Because the same electric currents give rise to local magnetic fields, simulating the magnetic fields provides an alternative method for mapping the nanobumps.

We acknowledge financial support from the EPSRC grant EP/G060649/1, the fund for scientific research Flanders (FWO-V), the KU Leuven (CREA, GOA), Methusalem Funding by the Flemish government, and the Belgian Inter-University Attraction Poles IAP Programmes. AVS was partially supported by "Crédit de démarrage," U.Lg. and "Mandat d'impulsion scientifique," FNRS. CR, NP, UZ, and BC acknowledge financial support from the Centre for Quantum Engineering and Space-Time Research (QUEST). CR and BC further acknowledge financial support by the German priority program SPP 1391 "Ultrafast Nanooptics" of the Deutsche Forschungsgemeinschaft (DFG) and the Laboratory of Nano and Quantum Engineering (LNQE) of the Leibniz University Hanover (LUH). CR and NP enjoyed fruitful discussions with Uwe Morgner.

References

1. X. Huang, W. Qian, I. H. El-Sayed, and M. A. El-Sayed, Lasers Surg. Med. **39**, 747 (2007).
2. K.-H. Dostert, M. Álvarez, K. Koynov, A. del Campo, H.-J. Butt, and M. Kreiter, Langmuir **28**, 3699 (2012).
3. C. J. Chen and R. M. Osgood, Phys. Rev. Lett. **50**, 1705 (1983).
4. J. B. Pendry, Contemp. Phys. **45**, 191 (2004).
5. V. G. Veselago, Sov. Phys. Usp. **10**, 509 (1968).
6. N. Engheta, Science **317**, 1698 (2007).
7. V. K. Valev, A. V. Silhanek, B. De Clercq, W. Gillijns, Y. Jeyaram, X. Zheng, V. Volskiy, O. A. Aktsipetrov, G. A. E. Vandenbosch, M. Ameloot, V. V. Moshchalkov, and T. Verbiest, Small **7**, 2573 (2011).
8. D. Schurig, J. J. Mock, B. J. Justice, S. A. Cummer, J. B. Pendry, A. F. Starr, and D. R. Smith, Science **314**, 977 (2006).
9. A. Grbic and G. V. Eleftheriades, Phys. Rev. Lett **92**, 117403 (2004).
10. N. Fang, H. Lee, C. Sun, and X. Zhang, Science **308**, 534 (2005).
11. E. J. R. Vesseur, R. de Waele, M. Kuttge, and A. Polman, Nano Lett. **7**, 2843 (2007).
12. J. Nelayah, M. Kociak, O. Stéphan, F. Javier, G. de Abajo, M. Tencé, L. Henrard, D. Taverna, I. Pastoriza-Santos, L. M. Liz-Marzán, and C. Colliex, Nat. Phys. **3**, 348 (2007).
13. R. Hillenbrand, F. Keilmann, P. Hanarp, D. S. Sutherland, and J. Aizpurua, Appl. Phys. Lett. **83**, 368 (2003).
14. V. K. Valev, A. V. Silhanek, Y. Jeyaram, D. Denkova, B. De Clercq, V. Petkov, X. Zheng, V. Volskiy, W. Gillijns, G. A. E. Vandenbosch, O. A. Aktsipetrov, M. Ameloot, V. V. Moshchalkov, and T. Verbiest, Phys. Rev. Lett. **106**, 226803 (2011).
15. V. K. Valev, D. Denkova, X. Zheng, A. I. Kuznetsov, C. Reinhardt, B. N. Chichkov, G. Tsutsumanova, E. J. Osley, V. Petkov, B. De Clercq, A. V. Silhanek, Y. Jeyaram, V. Volskiy, P. A. Warburton, G. A. E. Vandenbosch, S. Russev, O. A. Aktsipetrov, M. Ameloot, V. V. Moshchalkov, and T. Verbiest, Adv. Mater. **24**, OP29 (2012).
16. V. K. Valev, X. Zheng, C. G. Biris, A. V. Silhanek, V. Volskiy, B. De Clercq, O. A. Aktsipetrov, M. Ameloot, N. C. Panoiu, G. A. E. Vandenbosch, and V. V. Moshchalkov, Opt. Mater. Express **1**, 36 (2011).
17. G. Baffou, C. Girard, and R. Quidant, Phys. Rev. Lett. **104**, 136805 (2010).
18. A. F. Oskooi, D. Roundy, M. Ibanescu, P. Bermel, J. Joannopoulos, and S. G. Johnson, Comput. Phys. Commun. **181**, 687 (2010).
19. D. S. Ivanov, B. Rethfeld, G. M. O'Conner, T. J. Glynn, A. N. Volkov, and L. V. Zhigilei, Appl. Phys. A **92**, 791 (2008).
20. A. I. Kuznetsov, C. Unger, J. Koch, and B. N. Chichkov, Appl. Phys. A **106**, 479 (2012).
21. The material file is from E. D. Palik, *Handbook of Optical Constants of Solids* (Academic, 1985).
22. Y. Schols and G. A. E. Vandenbosch, IEEE Trans. Antennas Propag. **55**, 1086 (2007).
23. G. A. E. Vandenbosch, V. Volski, N. Verellen, and V. V. Moshchalkov, Radio Sci. **46**, RS0E02 (2011).